

A New Directional Filter Bank for 3D Texture Segmentation: Application to Lamellar Microstructure in Titanium Alloys

Laurent>About

Institute of Applied Computer Science, Lodz University of Technology, Poland

Laurent.babout@p.lodz.pl

Lukasz Jopek

Institute of Applied Computer Science, Lodz University of Technology, Poland

ljopek@kis.p.lodz.pl

Marcin Janaszewski

Institute of Applied Computer Science, Lodz University of Technology, Poland

janasz@kis.p.lodz.pl

Abstract

The paper presents the methodology used to design and implement a new 3D filter, called the CHG filter (Complementary of HourGlass) and the corresponding directional filter bank to detect surface-like singularities in 3D images. This is used for the application of segmenting lamellar colonies in tomographic images of titanium alloy for further microstructural characterization.

1. Introduction

There has been a significant increase of development of 3D image processing and analysis methods in the past decade due to the increased number of X-ray microtomography applications, especially in the field of materials science. Most of the proposed methods relied on well-known algorithms, mainly developed in a first stage for medical needs. However, one can cite recent works, which have necessitated the development or modification of 3D image processing approaches to solve specific materials science problems, such as the extraction of bridges along crack using the hole filling algorithm [1,2] or the quantification of pore interconnectivity in tissue scaffold based on the watershed method [3].

Similarly, the current work aims at proposing an image processing methodology to segment lamellar colonies in ($\alpha+\beta$) titanium (Ti) alloys. This type of microstructure consists of a group of α -colonies, roughly corresponding to parallel planes equally spaced, which have grown in different directions inside β grains. In 2D, this has similarity, in some extent, with highly magnified areal photos of roads (the β grain boundaries) surrounded by agricultural tilled fields (the α -colonies). Few approaches have been tested to segment lamellar colonies, including gradient-based method on 3D images [4], separable wavelet-based method [5] or the Bamberger directional filter bank (BDFB) [6] defined in the contourlet method [7] on 2D images. While the two first approaches have shown important limits in segmenting the colonies, the latter have shown promising results, due to the decomposition of the frequency space using fan filter banks. A N-D version, called the surfacelet transform [8], which uses multidimensional directional filter bank based on the hourglass shape, is able to capture

surface-like singularities for further denoising steps. Note that the approach was rather thought for denoising video sequences rather than segmenting 3D images.

This paper is somehow inspired from the previously mentioned method, where a 3D filter bank defined in the spatial domain has been designed to capture surface-like features of different directionalities, such as in the case of the titanium lamellar microstructure. The following structure of the paper presents the design and implementation of this filter bank, followed by the main algorithm implementing it to classify colonies into a finite number of direction-based objects. The approach is tested on X-ray microtomographic images of Ti alloy. Despite being developed for this particular application, the approach could be also used for other material science aspects, such as study of crack bifurcation. It could be also applied to any task where one aims at the recognition of noisy texture, which reveals directional properties via a set of curves in 2D or set of surfaces in 3D.

2. 3D filter design and implementation

The detection of lamellar colonies needs the development of a dedicated directional filter bank (DFB) so as to retrieve the changes of colony orientation and to delineate boundaries. Since lamellar colonies in 3D are, in a first approximation, equivalent to uniformly spaced and parallel planar objects, the directionality of the features can be retrieved using a 3D filter, which holds the following properties:

- cylindrical symmetry
- wedge-shape support

The filter shown in Figure 1 satisfies these conditions. The hourglass filter, which is appropriate for detecting 3D lines, is the complementary part of the presented filter, which is named CHG (Complementary part of HourGlass filter).

Given the cubic filter $CHG: \{0, 1, \dots, 2w+1\}^3 \rightarrow \{0, 1\}$ of half-size w , the wedge half-angle α and the vector \mathbf{n} , the filter shape can be built using the following pseudo-code:

Algorithm 1. Build CHG(Input w, α, \mathbf{n} , Output CHG)

01. $c := (w+1, w+1, w+1)$

02. Calculate $S = \{p \in Z^3 : D_E(p, c) \leq w\}$

03. Calculate $P = \{p \in S : \mathbf{n} \times (p - c) = 0\}$

04. $\forall x \in P, CHG(x) := 1$

-
05. Calculate $C = \{p \in S \setminus P : D_E(p, P) \leq (w+1)\tan(\alpha)\}$
06. **For each** voxel p in C
07. $\theta := \pi - \cos^{-1}(\frac{((\mathbf{p} - \mathbf{c}) \cdot \mathbf{n})}{\|\mathbf{p} - \mathbf{c}\| \|\mathbf{n}\|})$
08. **If** $\theta < \pi/2 - \alpha$ **Or** $\theta > \pi/2 + \alpha$
09. $CHG(p) := 1$
-

The above algorithm works as follows. First a sphere S of radius w at central point c of the original volume is defined (line 02) based on the Euclidean distance metric D_E . Then only voxels on the plane P with normal vector \mathbf{n} and containing central point c are selected (line 03). Every vectors starting at c , which have their projection angle upon the plane P lower than α , are further kept to build the filter (lines 06-09). Line 05 only guarantees that not all the points defining the sphere S are used for the calculation so as to reduce the processing time.

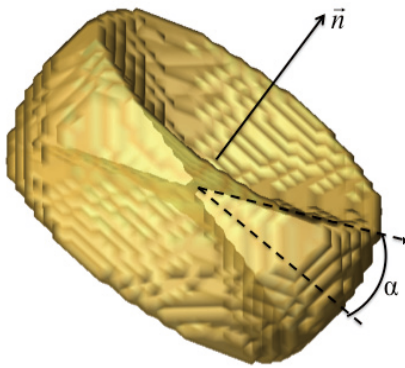


Figure 1. Isosurface of the CHG filter.

In order to have a filter that accepts fluctuations for planes with their normal vector in the vicinity of the vector defining the main direction of the filter, a planar symmetric univariate kernel, which has a similar construction to the Epanechnikov kernel [9] is used, having the profile

$$k(\theta_{\mathbf{u}}) = \begin{cases} 1 - \theta_{\mathbf{u}}/\alpha, & \text{if } 0 \leq \theta_{\mathbf{u}} \leq \alpha \\ 0, & \text{if } \theta_{\mathbf{u}} > \alpha \end{cases} \quad (1)$$

where $\theta_{\mathbf{u}}$ is the projection angle of any vector \mathbf{u} onto the plane P . However, the above expression is only true for vectors having their norm lower than the filter half-size w . A 2D illustration of such kernel for the direction $[001]$ is shown in Figure 2. As one can see, there is only an angular linear decay towards larger angles from the central plane, as the kernel profile is radially invariant in its current form.

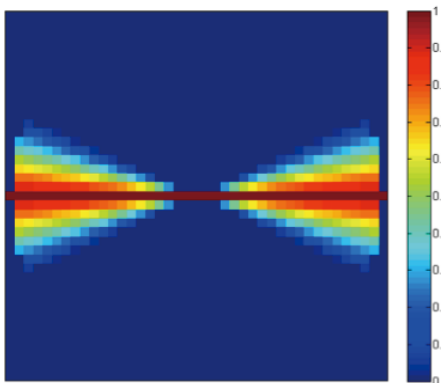


Figure 2. 2D filter kernel profile.

The kernel profile is further used in the kernel expression

$$K(p) = c_k K(\theta_{\mathbf{p}-\mathbf{c}}) \quad (2)$$

with

$$c_k = \sum_{i=1}^n k(\theta_{\mathbf{p}_i-\mathbf{c}}) \quad (3)$$

a normalization factor taking into account the n data points defining the 3-dimensional filter space.

The next step concerns the construction of the filter bank. In the approach proposed in [8], the checkboard filter bank has been used to partition the 3D frequency space into component filters (called surfacelets) with rectangular-based pyramid shape radiating out from the origin. Back to the spatial domain, the surfacelets have oblate shapes, which indicate a strong filtering response to a specific normal direction of surface-like objects. In the present case, because of the specific shape of the CHG filter, passbands may overlap for directions of neighbored partitioning. This depends on the value of the wedge half-angle α . In that context, a slightly different approach is proposed in this paper. A set of normal directions \mathbf{n} is defined, based on the vertices, edges and faces of the Cartesian cubic grid. More specifically, the family of normal directions $\langle 100 \rangle$, $\langle 110 \rangle$ and $\langle 111 \rangle$ (following the crystallographic plane and direction notations) regroup 13 independent directions, which are further called the principal directions of the 3D directional filter bank. Their spatial representation is shown in Figure 3.

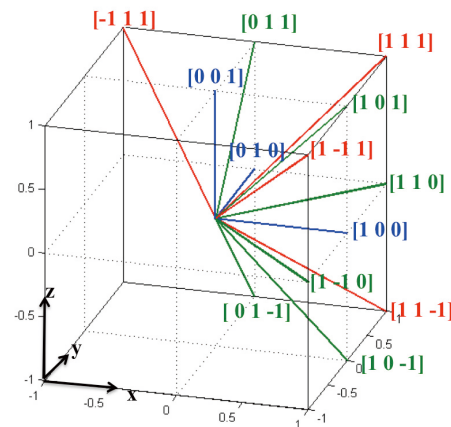


Figure 3. Bank of principal filter normal directions.

The filter response based on the kernel profile defined in equations (1-2) for the principal directions can also be presented using a spherical-polar representation, in order to analyse the effect of the choice of α to cover the 3D space. This is shown in Figure 4 for two values of α (i.e. $\pi/8$ and $\pi/4$). In the case of $\alpha = \pi/8$, one can see that regions of 0-value (i.e. blue (dark) areas) between filters of normal directions e.g. $[100]$, $[101]$ and $[111]$ are present, meaning that potential surface-like singularities perpendicular to these regions of directions will not be detected with the current DFB. Similarly, two directional filters may have a very similar local response, if the local direction is situated at the vicinity where passbands merge (e.g. at value 0.6 between filter directions $[110]$ and $[111]$ in Figure 4b). In that context, a second bank of

directions, called secondary directions and involving the family of normal directions $\langle 121 \rangle$, may be taken into account. However, this not is implemented in the current version of the proposed approach.

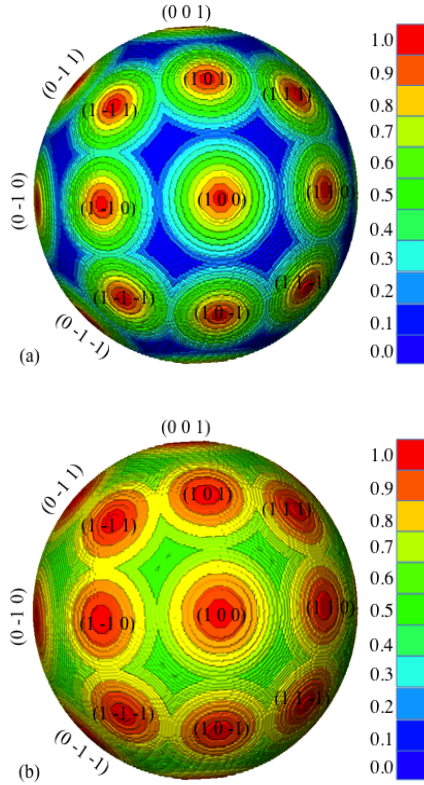


Figure 4. Polar representation of the filters' response
(a) $\alpha=\pi/8$ (b) $\alpha=\pi/4$.

3. Texture classification

Let consider the Definition domain $\Delta(N_1, N_2, N_3) = \{1, 2, \dots, N_1\} \times \{1, 2, \dots, N_2\} \times \{1, 2, \dots, N_3\}$ of an input volumetric image $I: \Delta(N_1, N_2, N_3) \rightarrow \{1, 2, \dots, 255\}$ and the directional filter bank \mathbf{g} based on the CGH filter as:

$$\mathbf{g} = (g_i)_{i=1,2,\dots,m} \quad (4)$$

where the indexation of the m directions is presented in Table 1 (in the present case, $m=13$).

Table 1. List of filter directions and corresponding classification indexes.

i	1	2	3	4	5
\mathbf{n}	[111]	[110]	[11-1]	[101]	[100]
i	6	7	8	9	10
\mathbf{n}	[10-1]	[1-11]	[1-10]	[-111]	[011]
i	11	12	13	-	-
\mathbf{n}	[010]	[01-1]	[001]	-	-

Let also define $D_E(p, q)$ and $D_C(p, q)$ the Euclidean and Chebyshev (Chessboard) distance metric. Finally, let define the matrix of ones h of size $(2r+1)^3$.

The output image $I_{cl}: \Delta(N_1, N_2, N_3) \rightarrow \{1, 2, \dots, m\}$ after classification is obtained from the following pseudo-code:

Algorithm 2. Classify(**Input** I, \mathbf{g}, h, m **Output** I_{cl})

01. $\forall p \in I, I(p) := I(p) I_{Otsu}(p)$
 02. Calculate $S = \{p \in I; I(p) > 0\}$
 03. $\forall i \in \{1, 2, \dots, m\}, f_i := I \otimes g_i$
 04. $\forall p \in S; I_{cl}(p) := \operatorname{argmax}_{i=1,2,\dots,m} (f_i(p))$
 05. $\forall i \in \{1, 2, \dots, m\}; f_i := f_i \otimes h$
 06. $\forall p \in S, I(p) := \operatorname{argmax}_{i=1,2,\dots,m} (f_i(p))$
 07. $\forall p \in S; I_{cl}(p) := I(p)$
 08. $\forall p \in I \setminus S; I_{cl}(p) := I\left(\operatorname{argmin}_{j \in S} (D_E(p, j))\right)$
-

In the algorithm above, *lines 01-02* assure that only feature points, which are selected from a segmentation step using the Otsu algorithm and defining the set S , are used for the direction filtering. In *lines 03-04*, convolution is performed between the previously filtered image and the m directional filters, and the index corresponding to the largest filter response for each point of S is used in the output image. Next, a denoising step, consisting in finding the mode between the convolution of the different segmented orientation classes and the operator h (matrix of 1), is used to locally compensate directional fluctuations in the image (*line 05-07*). The denoising rate relies upon the choice of the size of the neighborhood (i.e. r). Note that this is equivalent to finding the mode of a histogram of the neighborhood around each voxel. However, the execution time of a convolution in Matlab is far more effective than performing histogram calculation. As an example, for $N_1=N_2=N_3=500$ and $r=12$, the convolution-based method lasts around 200 s and is about 200 times faster than the histogram-based method (with the computer properties specified at the end of Section 4). Finally, the remaining points of the input image not belonging to S are assigned with the class index of the closest point from S (*line 08*).

4. Results: classification of lamellar colonies

The previous methodology combining 3DFB with texture classification is applied to the case of feature extraction, i.e. lamellar colonies, in microtomographic images of titanium alloy. Despite being developed for this particular application, the approach could be also used for other material science aspects, such as study of crack bifurcation. A 3D example of the microstructure is shown on Figure 5a. The image size is $270 \times 270 \times 270$ voxels. One can clearly notice groups of oriented surface-life features (seen as lines on each principal planes), each colony having random orientation. Lines have been drawn on the colony boundaries to help distinguishing them. One can also see that colony may be well defined along one visualization plane, but fading in an orthogonal one, as indicated by the arrows on Figure 5a. This confirms the use of a 3D method over 2D traditional one to detect surface-like singularities.

Figure 5b presents an exemplar result of the classifi-

cation method for the following input parameters: $w=10$, $\alpha=\pi/8$, $r=12$ and $m=13$ as mentioned previously. One can see that the different colonies, which could be detected visually, are, in most cases, satisfyingly classified using the proposed approach and the boundaries. The image reveals the presence of 5 main colonies of different orientations, which are in agreement with the guessed orientations. Indeed, as an example, colonies of orientation [010] and [001] are in agreement with orientation of the lamellae in the corresponding Cartesian coordinate system. The main problems reside in accurate colony boundary detection, as well as the presence of “noisy” class objects in large colonies, mainly resulting from the dual effects of the denoising and distance-based classification steps of algorithm 2. Comparison using the Figure Of Merit (FOM) proposed by Pratt [10] between a set of 2D images of the boundaries selected using manual segmentation (as shown in Figure 5) and the proposed directional classification shows that about 62% of the boundaries between colonies are well recovered in average. Note that the results based on BDFB used in the contourlet method [7] are, in average, 8% less (in that case, *line 03* of algorithm 2 is changed). The initial binarization step used to enhance lamellar also influences the boundary delineation. Results are considered promising and work is in progress to get a more robust classification method, as well as a deeper analysis of the effect of the input parameters on the classification results.

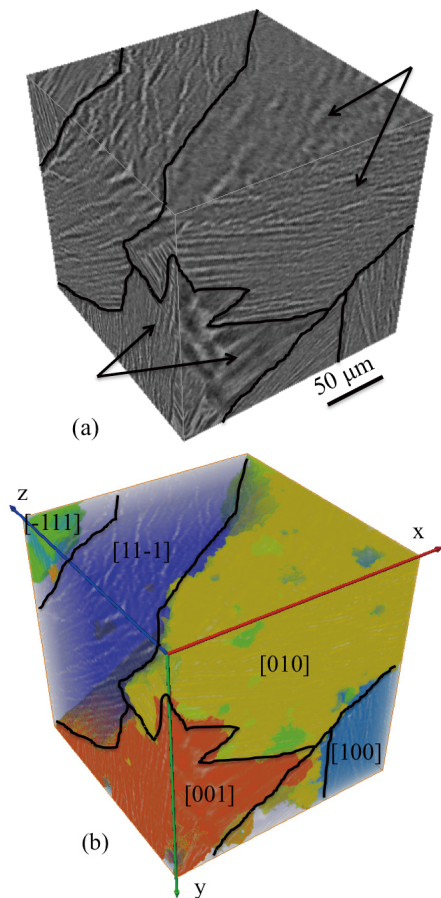


Figure 5. (a) X-ray microtomography image of lamellar microstructure in Ti alloy, together with manually drawn colony boundaries. (b) Superposition of the classification result.

The algorithm has been implemented in Matlab R2012a. The execution time is less than a minute for an initial input volume of size 270^3 on a server with the following specifications: 2 Intel Xeon processors (2.53 GHz), 24GB RAM, Windows XP 64bit.

5. Conclusion

The current paper has presented a trivial, but promising method to segment lamellar colonies in Ti alloy based on a new type of 3D directional filter bank. The following classification method allows to accurately retrieve the correct direction of the colonies, while the main problem concerns boundary delineation. The current method is a promising baseline for further improvement. The method seems to outperform filtering using Bamberger directional filter bank.

Acknowledgments: The work is supported by the Polish National Science Centre (grant no: 6522/B/T02/2011/40).

References

- [1] M. Janaszewski, et al.: "Hole filling in 3D volumetric objects," *Pattern Recognition*, vol.43, no.10, pp.3548-3559, 2010.
- [2] L. Babout, et al.: "A method for the 3-D quantification of bridging ligaments during crack propagation," *Scripta Materialia*, vol.65, no.2, pp.131-134, 2011.
- [3] J. R. Jones, et al.: "Non-destructive quantitative 3D analysis for the optimisation of tissue scaffolds," *Biomaterials*, vol.28, no.7, pp.1404-1413, 2007.
- [4] D. Jeulin, M. Moreaud: "Segmentation of 2d and 3d textures from estimates of the local orientation," *Image Analysis and Stereology*, vol.27, pp.183-192, 2008.
- [5] L. Babout, et al.: "Towards The Texture Segmentation Of X-Ray Tomography Images Of Lamellar Microstructure In Titanium Based Alloys," In 5th International Symposium on Process Tomography. Zakopane, Poland. 2008.
- [6] L. Jopek, et al.: "A new method to segment X-ray microtomography images of lamellar titanium alloy based on directional filter banks and gray level gradient," In International Conference on Computer Vision and Graphics (ICCVG 2010). Warsaw, Poland. 2012.
- [7] A. L. da Cunha, et al.: "The nonsubsamped contourlet transform: Theory, design, and applications," *IEEE Transactions on Image Processing*, vol.15, pp.3089-3101, 2006.
- [8] Y. M. Lu, M. N. Do: "Multidimensional directional filter banks and surfacelets," *IEEE Transactions on Image Processing*, vol.16, 2007.
- [9] D. Comaniciu, P. Meer: "Mean shift: A robust approach toward feature space analysis," *IEEE Transactions on Pattern Analysis and Machine Intelligence*, vol.24, no.5, pp.603-619, 2002.
- [10] W. K. Pratt, 2007. *Digital Image Processing*. New Jersey: Wiley.